413-nm lasers, respectively. Cells were sequentially illuminated with the 514- and 413-nm lasers so that all three signals could be detected from each cell. Compensation was applied so that there was no FRET signal visible from cells transfected with CFP or YFP alone. We collected 50,000 events from each sample and analyzed the data with the FlowJo software package (Treestar Inc.). Another characteristic of FRET is the dequenching of donor fluorescence after photobleaching of the acceptor. This dequenching can be converted to a measurement of FRET efficiency (E%), which is related to the distance between two molecules by the Förster equation [see (*23*)]. For FRET efficiency measurements, CFP emission intensities from cotransfected cells were measured on a fluorescence microscope before and after bleaching the YFP with 5 min of illumination through a 505- to 545-nm bandpass filter. We corrected for direct bleaching of cells transfected with the CFP fusion partner alone. FRET efficiencies were calculated using the formula E% = [1 − (CFP emission before YFP bleach/CFP emission after YFP bleach)] × 100%.

25. M. P. Boldin *et al.*, *J. Biol. Chem.* **270**, 387 (1995).
26. I. Herskowitz, *Nature* **329**, 219 (1987).
27. M. P. Cosma, M. Cardone, F. Carlomagno, V. Colantuoni, *Mol. Cell. Biol.* **18**, 3321 (1998); E. Jouanguy *et al.*, *Nature Genet.* **21**, 370 (1999); R. Levy-Toledano, L. H. Caro, D. Accili, S. I. Taylor, *EMBO J.* **13**, 835 (1994).
28. G. Papoff *et al.*, *J. Biol. Chem.* **274**, 38241 (1999); G. Papoff *et al.*, *J. Immunol.* **156**, 4622 (1996).
29. 293T cells were transfected with Fugene 6 (Boehringer Mannheim) according to the manufacturer's instructions. Cells were lysed in 150 mM NaCl, 20 mM tris-Cl (pH 7.5), 1 mM EDTA, 5 mM iodoacetamide, 2 mM dithiothreitol, 10% glycerol, 1% Triton X-100, and protease inhibitors (Boehringer Mannheim). After preclearing with protein G–agarose beads (Boehringer Mannheim) and normal mouse immunoglobulin G, proteins were immunoprecipitated with 1 mg anti-GFP (Roche Molecular Biochemicals) and protein G–agarose beads. Immune complexes were washed three times with lysis buffer. AU-1 was immunoprecipitated with 2 μl of anti–AU-1 (Covance) and protein A beads. Proteins were electrophoresed on Tris/Glycine gels (Novex), transferred to nitrocellulose membranes, and blotted with the indicated antibodies. Bands were visualized with SuperSignal WestDura (Pierce). Densitometry was performed with one-dimensional image analysis software (Kodak).
30. N. P. Mahajan, D. C. Harrison-Shostak, J. Michaux, B. Herman, *Chem. Biol.* **6**, 401 (1999).
31. We thank D. Martin, L. Zheng, and D. Smith for plasmid construction; K. Holmes, R. Swofford, and D. Stephany for excellent technical assistance; M. Peter and B. Herman for valuable reagents; T. Waldmann, R. Germain, H. Metzger, J. O'Shea, C. Jackson, and F. Hornung for critical reading of the manuscript and helpful comments; and S. Starnes for editorial assistance. S. Straus, J. Puck, C. Jackson, and J. Dale of the NIH ALPS working group provided clinical material and encouragement that were essential for this work. Supported by a Cancer Research Institute/Miriam and Benedict Wolf fellowship (F.K.-M.C.), NIH grant NS27177 (R.Y.T.), and a fellowship in the HHMI/NIH scholar program (M.J.).

28 December 1999; accepted 21 April 2000

Cross Talk Between Interferon-γ and -α/β Signaling Components in Caveolar Membrane Domains

Akinori Takaoka,[1] Yukiko Mitani,[1] Hirofumi Suemori,[2] Mitsuharu Sato,[1] Taeko Yokochi,[1] Shigeru Noguchi,[2] Nobuyuki Tanaka,[1] Tadatsugu Taniguchi[1]*

Definition of cellular responses to cytokines often involves cross-communication through their respective receptors. Here, signaling by interferon-γ (IFN-γ) is shown to depend on the IFN-α/β receptor components. Although these IFNs transmit signals through distinct receptor complexes, the IFN-α/β receptor component, IFNAR1, facilitates efficient assembly of IFN-γ–activated transcription factors. This cross talk is contingent on a constitutive subthreshold IFN-α/β signaling and the association between the two nonligand-binding receptor components, IFNAR1 and IFNGR2, in the caveolar membrane domains. This aspect of signaling cross talk by IFNs may apply to other cytokines.

The cytokines IFN-α/β and IFN-γ play central roles in the innate immune response against viral infections (*1–4*). IFN-γ is also widely involved in the regulation of adaptive immune responses (*5*). These cytokines transmit signals to the cell interior through distinct receptor complexes, the IFN-α/β receptor (IFNAR) and the IFN-γ receptor (IFNGR), each composed of two type II membrane glycoproteins: IFNAR1 and IFNAR2, and IFNGR1 and IFNGR2 (*2–4*, *6–8*). Ligand-induced stimulation of each IFN receptor complex results in the activation of the receptor-associated Janus protein tyrosine kinases (Jak PTKs), specifically, Jak1 and Tyk2 PTKs for IFNAR and Jak1 and Jak2 PTKs for IFNGR (*6–10*). After activation of these Jak PTKs, the signal transducers and activators of transcription 1 (Stat1) and Stat2 are tyrosine-phosphorylated, leading to formation of the two transcriptional activators, IFN-γ–activated factor (GAF)/IFN-α–activated factor (AAF) and IFN-stimulated gene factor 3 (ISGF3)/Stat1-p48 (*9*, *11*). Although IFN-α/β and IFN-γ elicit cellular antiviral activities, it is unknown whether IFNAR and IFNGR share any functional aspects in the signaling processes. Receptors for these IFNs and other cytokines are expressed at low levels, ranging from 10^2 to 10^3 molecules on the cell surface (*2*), but can efficiently transmit signals to the cell interior. This raises the possibility that these receptors are clustered, even before ligand stimulation, to a particular region of the cell membrane.

Mouse embryonic fibroblasts (MEFs), isolated from either IFNAR1-deficient or IFNGR1-deficient mice (*12*, *13*), were examined for their antiviral response induced by IFN-γ or IFN-α (*14*). In MEFs lacking IFNAR1 (IFNAR1-null MEFs) (*15*), the IFN-γ–induced antiviral response was impaired; a concentration of IFN-γ that was 10 times higher than that for wild-type (WT) MEFs was required to achieve 50% protection of the cells from encephalomyocarditis virus (EMCV) infection, and full IFN-γ response was not achieved at even higher ligand concentrations (Fig. 1A). In contrast, the IFN-α–induced antiviral response was normal in MEFs deficient in IFN-γ receptor (IFNGR1-null MEFs). The IFN-γ–induced DNA-binding activity of Stat1 was six to seven times lower in IFNAR1-null MEFs than in WT MEFs (Fig. 1B) (*12*), although the kinetics of the Stat1 activation was the same (*16*). Similar results were obtained in splenocytes of these mutant mice (*16*), indicating that the observed defect in Stat1 activation is not restricted to MEFs. In contrast, Stat1 activation by IFN-α was normal in IFNGR1-null MEFs (*16*), consistent with the antiviral assay result. Like IFN-α/β stimulation, IFN-γ stimulation activates ISGF3 in MEFs (*17*), which is critical for the IFN-γ–induced antiviral response (*17*, *18*). In IFNAR1-null MEFs, however, IFN-γ–induced formation of the ISGF3 complex was not detected (Fig. 1B).

To determine the role of IFNAR1 in IFN-γ signaling, we expressed mutant forms of IFNAR1 (Fig. 1C) in the IFNAR1-null MEFs. Expression of WT IFNAR1 restored the IFN-γ–induced activation of Stat1 and ISGF3 (Fig. 1C, lower panel), as well as antiviral responses (Fig. 1D). However, expression of either a mutant IFNAR1 lacking the cytoplasmic region or a chimeric receptor composed of the IFNAR1 transmembrane and cytoplasmic region failed to restore the response to IFN-γ (Fig. 1, C and D).

These results raised the question of whether an intact IFNAR1 or an IFN-α/β signaling event, mediated by IFNAR1, is required to produce a complete IFN-γ response. Because low levels of IFN-α/β mRNA expression were detected by reverse

[1]Department of Immunology, Graduate School of Medicine and Faculty of Medicine, University of Tokyo, Hongo 7-3-1, Bunkyo-ku, Tokyo 113-0033, Japan. [2]Meiji Institute of Health Science, Meiji Milk Products, Naruda 540, Odawara-shi, Kanagawa 250-0862, Japan.

*To whom correspondence should be addressed. E-mail: tada@m.u-tokyo.ac.jp

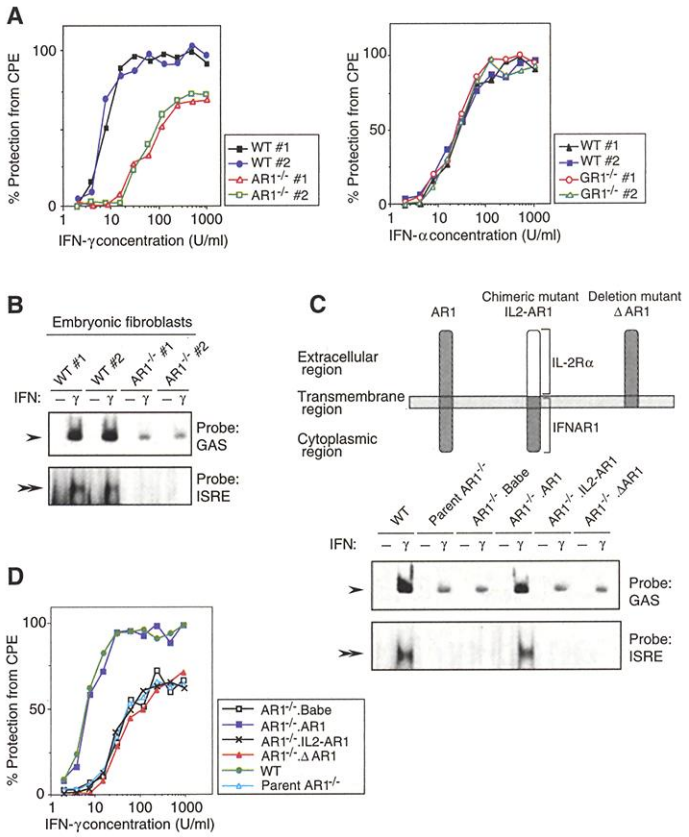

Fig. 1. Impaired antiviral response and DNA-binding activity of Stat1 induced by IFN-γ in IFNAR1-null cells. (**A**) Antiviral activity of IFN-γ or IFN-α in IFNAR1-null (AR1$^{-/-}$, left), IFNGR1-null (GR1$^{-/-}$, right), or wild-type (WT, left and right) MEFs. Two cell clones derived from the same littermates, indicated as #1 and #2, were randomly selected (*31*, *32*). The cytopathic effect (CPE) of EMCV (multiplicity of infectivity = 0.1) was quantified as described (*31*, *32*). Indicated values are the means of triplicate experiments. The standard deviation of the measurements was within ±15% in each assay. (**B**) IFN-γ–induced DNA-binding activities of Stat1 and ISGF3 in WT and AR1$^{-/-}$ MEFs. Cells were untreated (−) or treated with IFN-γ (γ), and subjected to electrophoretic mobility shift assay (EMSA) with a ^{32}P-labeled oligonucleotide probe, comprising either the *interferon regulatory factor−1* (*IRF-1*)–IFN-γ–activated site (GAS) or the *2′,5′oligoadenylate synthetase* (*2′,5′OAS*)–IFN-stimulated responsive element (ISRE) (*33*). The positions of the IFN-γ–induced DNA-binding complex are indicated by arrows. The identity of these complexes was confirmed by their reactivity to anti-Stat1 or anti-Stat2 (*16*). The quantification analysis revealed that ISRE induction level by IFN-γ at 250 U/ml corresponded approximately to the induction level by IFN-α at 15 U/ml (*19*). (**C**) A schematic representation (upper panel) of the WT (AR1) and two mutant forms of IFNAR1 (IL2-AR1 or ΔAR1), and IFN-γ–induced DNA-binding activity of Stat1 in WT, parental IFNAR1-null MEFs (Parent AR1$^{-/-}$), or IFNAR1-null MEFs transfected with control vector (AR1$^{-/-}$.Babe), the WT (AR1$^{-/-}$.AR1), or two mutant forms of IFNAR1 (AR1$^{-/-}$.IL2-AR1 or AR1$^{-/-}$.ΔAR1). Each construct was cloned into a retrovirus vector, pBabe-puro, and the retrovirus-mediated gene transfers were performed as described (*31*). The ^{32}P-labeled *IRF-1*–GAS or *2′,5′OAS*-ISRE probe was used in the EMSA. (**D**) IFN-γ–induced antiviral activity in MEFs expressing the WT and mutant forms of IFNAR1, as described in (A).

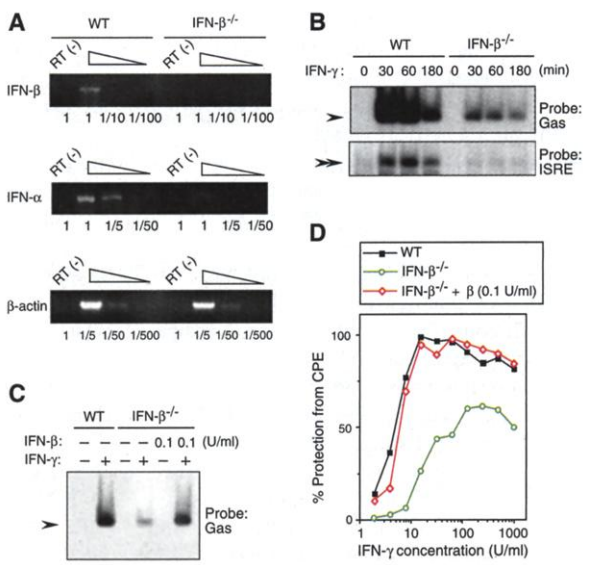

Fig. 2. Requirement of IFN-α/β signaling for effective IFN-γ signaling. (**A**) Expression of IFN-β and IFN-α's mRNA was analyzed by RT-PCR in wild-type (WT) and IFN-β–null MEFs (IFN-β$^{-/-}$) (*18*). Values of the dilution rates for PCR templates after the first-strand synthesis are indicated below each lane. The same samples were analyzed by RT-PCR with β-actin primers as control. RNA samples without the first-strand reaction were also subjected to PCR amplification [RT(−)]. (**B**) Kinetics of DNA-binding activity of Stat1 stimulated by IFN-γ in WT and IFN-β$^{-/-}$ MEFs. A ^{32}P-labeled oligonucleotide probe comprising the *IRF-1*–GAS or the *2′,5′OAS*-ISRE was used in the EMSAs. (**C**) IFN-γ–induced DNA-binding activity of Stat1 in WT or IFN-β$^{-/-}$ MEFs in the presence or absence of a low concentration of IFN-β (0.1 U/ml). After a 1-hour incubation with IFN-β (0.1 U/ml), MEFs were additionally treated with IFN-γ (250 U/ml) and subjected to EMSA (*33*). Essentially the same observation was made with IFN-α (0.1 U/ml) (*19*). (**D**) IFN-γ–induced antiviral response of WT or IFN-β$^{-/-}$ MEFs in the presence or absence of a low concentration of IFN-β (0.1 U/ml).

transcriptase–polymerase chain reaction (RT-PCR) in MEFs, splenocytes, and other tissues of the mouse [Fig. 2A and (*16*)], mice were generated that carry a nullizygosity in the *IFN*-β gene (*19*), based on the dependence of IFN-α production on IFN-β production in MEFs (*20*, *21*). Indeed, IFN-α mRNA expression was not detected by RT-PCR in the *IFN*-β–deficient MEFs (IFN-β–null MEFs) (Fig. 2A). IFN-β–null MEFs also showed a deficiency in IFN-γ–induced Stat1 activation (Fig. 2B) and antiviral response (Fig. 2D). This deficiency was rescued by an exogenously added IFN-β at low concentration (0.1 U/ml), which by itself did not activate Stat1 (Fig. 2C). A similar effect was observed after the addition of antibodies to IFN-α/β (anti–IFN-α/β) to the WT MEFs (*19*), further indicating the importance of a constitutive subthreshold IFN-α/β signaling, in the absence of virus infection, for the full IFN-γ response.

To further investigate the mechanism by which IFN-α/β signaling contributes to IFN-γ signaling, we determined IFN-γ–induced tyrosine phosphorylation levels of Jak1 and Jak2, and of their target molecule, Stat1. Although the levels remained unaffected in IFNAR1-null MEFs (*16*), glycerol gradient fractionation analysis of cell extracts revealed that the amount of fast-sedimenting fractions of Stat1 (Fig. 3A), representing the dimeric form (*22*), was smaller in the extract from the IFN-γ–stimulated IFNAR1-null MEFs than in extracts from IFN-γ–stimulated WT MEFs (Fig. 3A). One possible reason for inefficient dimerization of Stat1 in IFNAR1-null MEFs could be that the IFNAR signaling complex, activated by constitutively produced IFN-α/β, provides a site for Stat1 to efficiently dimerize upon tyrosine phosphorylation by IFN-γ. Phosphorylated tyrosine residue 466 (Y466) of human IFNAR1 mediates the association of Stat1 with IFNAR1, a recruitment that is probably dependent on Stat2 (*23*, *24*). Likewise, the tyrosine residue 440 (Y440) of human IFNGR1 also binds to Stat1 (*25*).

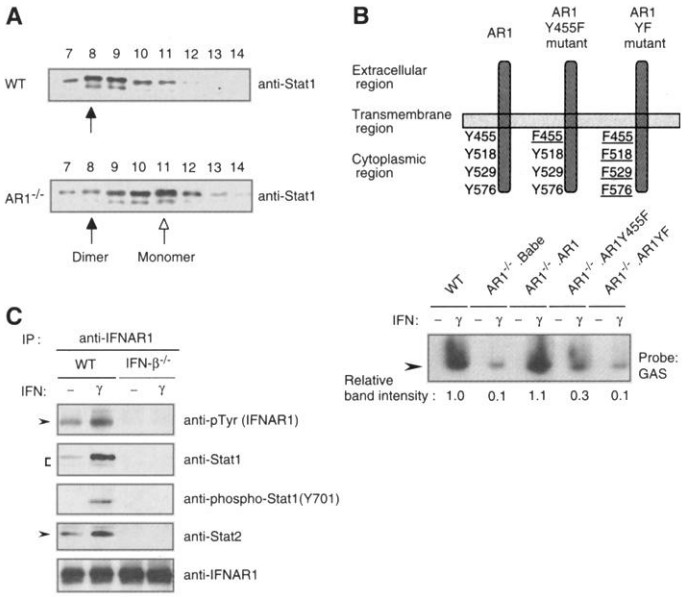

Fig. 3. Involvement of IFNAR1 in efficient dimerization of the IFN-γ–activated Stat1. (**A**) Formation of Stat1 dimer as determined by glycerol gradient analysis. Extracts from IFN-γ–treated (250 U/ml, 30 min) WT or AR1$^{-/-}$ MEFs were subjected to centrifugation through 10 to 40% glycerol gradients for 36 hours at 274,000*g* in an SW41 rotor (Beckman) as described (*22*). Fractions 7 to 14 from the gradient were separated by 7.5% SDS–polyacrylamide gel electrophoresis, followed by immunoblotting with antibody to Stat1 (anti-Stat1) (*34*). Peaks of Stat1 dimer or Stat1 monomer are indicated by a closed or open arrow, respectively. (**B**) Effect of the mutations in the tyrosine residues of IFNAR1 on the IFN-γ–induced DNA-binding activity of Stat1. A schematic representation (upper panel) of the WT (AR1) and mutant forms of murine IFNAR1 [AR1Y455F, substitution of tyrosine at position 455 by phenylalanine; AR1YF, substitution of all intracellular tyrosines (455, 518, 529, and 576) by phenylalanine]. EMSA (lower panel) was done with untreated (−) or IFN-γ–treated (γ) cell extracts from the following MEFs: wild-type MEFs (WT); IFNAR1-null MEFs transfected with control vector (AR1$^{-/-}$.Babe); or IFNAR1-null MEFs expressing AR1 (AR1$^{-/-}$.AR1), AR1Y455F mutant (AR1$^{-/-}$.AR1Y455F), or AR1YF mutant (AR1$^{-/-}$.AR1YF). ^{32}P-labeled *IRF-1*–GAS probe was used. The values below represent the relative intensities of the corresponding bands as quantified with the image analyzer (BAS5000, Fujix). (**C**) Tyrosine-phosphorylated Stat1 is associated with IFNAR1 after IFN-γ treatment (250 U/ml). Immunoblots of anti-IFNAR1 immunoprecipitates with cell lysates prepared from WT and IFN-β$^{-/-}$ MEFs untreated (−) or treated with IFN-γ (γ) (*34*), anti-phosphotyrosine, anti-Stat1, anti–Tyr^{701}-phosphorylated Stat1, anti-Stat2, or anti-IFNAR1.

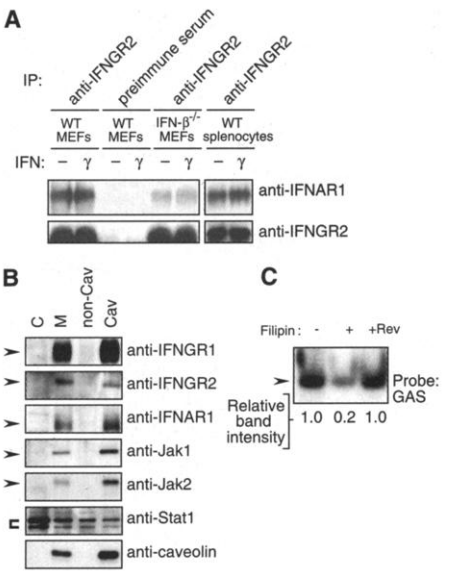

Fig. 4. Association of IFNAR1 with IFNGR2 in caveolar membrane domains. (**A**) Coimmunoprecipitation of IFNAR1 with IFNGR2. WT MEFs, WT splenocytes, and IFN-β$^{-/-}$ MEFs were untreated (−) or treated with IFN-γ (γ), and cell lysates were subjected to immunoprecipitation (*34*). Anti-IFNAR1 (upper panel) and anti-IFNGR2 (lower panel) immunoblots of anti-IFNGR2 immunoprecipitates. Preimmune rabbit serum was used as a negative control. Immunoprecipitation analysis revealed that IFNAR1 protein that associated with IFNGR2 was ~80% of the total IFNAR1 protein (*16*). (**B**) Selective localization of IFNAR and IFNGR subunits, and Jak PTKs, in caveolar membrane domains. The caveolar membrane fraction from WT MEFs was prepared by the detergent-free method (*30*). Extracts containing 5 μg of total protein from the four cellular compartments (cytosol, C; plasma membrane, M; noncaveolar fractions, non-Cav; and caveolar fractions, Cav) were loaded onto each lane and analyzed by immunoblotting with the indicated antibodies (*34*). (**C**) Reversible inhibition of IFN-γ–induced DNA-binding activity of Stat1 in filipin-treated WT MEFs. Filipin-untreated (−) or -treated (+) WT MEFs were stimulated with IFN-γ (100 U/ml) and subjected to EMSA. +Rev (lane 3) represents the result obtained after reversing the filipin effects (*30*). The relative band intensities quantified with the imaging analyzer (BAS5000, Fujix) are shown below.

Ectopic expression of a mutant murine IFNAR1 (AR1Y455F) resulted in only about 20% restoration of IFN-γ–induced activation of Stat1, as compared with full restoration by WT IFNAR1, despite similar receptor expression levels in IFNAR1-null MEFs (Fig. 3B) (*16*). This result suggests a major role for this tyrosine residue in Stat1 recruitment. The IFNAR1 mutant with mutations in all four intracellular tyrosine residues (AR1YF) was completely inactive (Fig. 3B). These results suggest that the subthreshold IFN-α/β signaling may be essential for maintaining IFNAR1 in a phosphorylated form, thereby providing a site for the IFN-γ–activated Stat1 to undergo efficient dimerization. Consistent with this notion is the observation that IFNAR1 is tyrosine-phosphorylated in the WT, but not in IFN-β–null MEFs (Fig. 3C). Because the phosphorylation of IFNAR1 was further increased by IFN-γ stimulation in WT MEFs, but not in IFN-β–null MEFs, IFNAR1 phosphorylation, with or without IFN-γ stimulation, may depend on IFN-α/β signaling.

Stat1 coimmunoprecipitated with IFNAR1, even in the absence of IFN-γ stimulation, in WT MEFs but not in IFN-β–null MEFs (Fig. 3C), indicating that IFNAR1 tyrosine phosphorylation is required for this association. However, IFNAR1-recruited Stat1 was not phosphorylated (Fig. 3C), suggesting that IFN-α/β signaling may have little, if any, effect on Stat1 phosphorylation. After IFN-γ stimulation, the association of phosphorylated Stat1 (*9*, *10*) with IFNAR1 was detected in the WT MEFs, but not in IFN-β–null MEFs (Fig. 3C). Stat2 recruitment to IFNAR1, found in the WT MEFs, also increased after IFN-γ stimulation (Fig. 3C).

In view of the cross talk between IFN-α/β and -γ signaling, in which the IFNAR1 phosphorylation and Stat1/Stat2 recruitment to IFNAR1 are enhanced by IFN-γ, IFNAR1 was examined for its association with the IFNGR. IFNAR1 coimmunoprecipitated with IFNGR2, the nonligand-binding component of the IFNGR complex, even before IFN-γ stimulation in WT MEFs and in splenocytes (Fig. 4A). This association was reduced in IFN-β–null MEFs (Fig. 4A), suggesting that IFN-α/β signaling may contribute to IFN-γ signaling through IFNAR1 association with IFNGR2.

Signaling cross talk between the two types of IFNs provides a molecular basis for their overlapping functions (*19*). The cross talk appears unidirectional in that IFN-γ signaling was dependent on IFN-α/β signaling, but not vice versa. Because IFNAR1 can provide efficient docking sites for Stat1 and Stat2, the IFNAR1-associated IFNGR2, for which no such docking sites have been reported, may not be required for IFN-α/β signaling. In this context, the IFN-γ system, which by itself can elicit a weak antiviral activity, may acquire more potent antiviral activity through utilization of the IFN-α/β system. This may also explain the previously reported synergism between IFN-α/β and IFN-γ (*2*, *26*, *27*). The results also suggest that the constitutive subthreshold IFN-α/β signaling has two major roles: to strengthen an otherwise weak association of IFNAR1 with IFNGR2 (Fig. 4A), and to maintain the docking sites in IFNAR1 for Stat1 (Fig. 3C).

The IFN receptor components tested were

shown to be exclusively localized in caveolar membrane fractions (Fig. 4B), which is characteristic of dynamic clustering of sphingolipids and cholesterol (*28*, *29*). Treatment of the cells by filipin, which disperses caveolar domains (*30*), resulted in a dose-dependent inhibition of Stat1 activation (*16*), and this inhibition was reversible (Fig. 4C), suggesting that the localization of IFNGR and IFNAR is critical for efficient signaling. The intracellular levels of Jak1 and Jak2 were also found to be concentrated in the caveolar membrane domains (Fig. 4B), suggesting that the caveolar domain–dependent signaling may be a feature shared by other cytokines that use these kinases for signaling. Local concentration of cytokine receptors at caveolar membrane may be important for efficient ligand-induced receptor oligomerization and cross talk among cytokine receptor components.

References and Notes

1. C. Weissmann and H. Weber, *Prog. Nucleic Acid Res. Mol. Biol.* **33**, 251 (1986).
2. E. DeMaeyer and J. DeMaeyer-Guignard, *Interferons and Other Regulatory Cytokines* (Wiley, New York, 1988).
3. J. Vilcek and G. S. Sen, in *Fields Virology*, D. M. Fields, P. M. Knipe, P. M. Howley, Eds. (Lippincott-Raven, Philadelphia, ed. 3, 1996), p. 375.
4. S. Pestka, J. A. Langer, K. C. Zoon, C. E. Samuel, *Annu. Rev. Biochem.* **56**, 727 (1987).
5. A. Billiau, *Adv. Immunol.* **62**, 61 (1996).
6. C. Schindler and J. E. Darnell Jr., *Annu. Rev. Biochem.* **64**, 621 (1995).
7. E. A. Bach, M. Aguet, R. D. Schreiber, *Annu. Rev. Immunol.* **15**, 563 (1997).
8. G. R. Stark, I. M. Kerr, B. R. Williams, R. H. Silverman, R. D. Schreiber, *Annu. Rev. Biochem.* **67**, 227 (1998).
9. J. E. Darnell Jr., I. M. Kerr, G. R. Stark, *Science* **264**, 1415 (1994).
10. J. N. Ihle and I. M. Kerr, *Trends Genet.* **11**, 69 (1995).
11. A. R. Bluyssen, J. E. Durbin, D. E. Levy, *Cytokine Growth Factor Rev.* **7**, 11 (1996).
12. The result of the antiviral assay presented in figure 2A of U. Müller *et al.* [*Science* **264**, 1918 (1994)] is consistent with our present results. To investigate further the extent to which the loss of IFNAR1 affects IFN-γ–induced gene expression, we examined the mRNA induction kinetics for *IRF-1* and *2′,5′OAS* genes by IFN-γ in the WT and IFNAR1-null MEFs. The induction of IRF-1 mRNA by IFN-γ was six times lower in the mutant MEFs than in the WT MEFs. We also examined the induction of *2′,5′OAS* mRNA, which is dependent on ISGF3, in the WT and IFNAR1-null MEFs. The induction of *2′,5′OAS* mRNA by IFN-γ remained undetectable in IFNAR1-null MEFs throughout the time course tested (*19*).
13. S. Huang *et al.*, *Science* **259**, 1742 (1993).
14. IFNAR1-deficient and IFNGR1-deficient mice were purchased from B&K Universal Group (North Humberside, UK). MEFs and splenocytes were prepared according to standard methods [A. Takaoka *et al.*, *EMBO J.* **18**, 2480 (1999)]. Recombinant murine IFN-γ was purchased from Genzyme/Techne.
15. Flow cytometry and immunoblot analyses revealed that the expression levels of IFNGR1 and IFNGR2 in these cells are essentially the same as in the WT MEFs. Immunoblot analysis showed that nearly the same amount of endogenous Stat1 protein was detected in the WT and IFNAR1-null MEFs.
16. A. Takaoka and Y. Mitani, unpublished data.
17. M. Matsumoto *et al.*, *Biol. Chem.* **380**, 699 (1999).
18. T. Kimura *et al.*, *Genes Cells* **1**, 115 (1996).
19. Supplemental Web material is available at *Science* Online at www.sciencemag.org/feature/data/1049334.shl.
20. M. Sato, unpublished results.
21. L. Erlandsson *et al.*, *Curr. Biol.* **8**, 223 (1998).
22. K. Shuai *et al.*, *Cell* **76**, 821 (1994).
23. X. Li, S. Leung, I. M. Kerr, G. R. Stark, *Mol. Cell. Biol.* **17**, 2048 (1997).
24. H. Yan *et al.*, *EMBO J.* **15**, 1064 (1996).
25. A. C. Greenlund, M. A. Farrar, B. L. Viviano, R. D. Schreiber, *EMBO J.* **13**, 1591 (1994).
26. W. R. Fleischmann Jr., J. A. Georgiades, L. C. Osborne, H. M. Johnson, *Infect. Immun.* **26**, 248 (1979).
27. W. E. Stewart II, L. B. Gosser, R. Z. Lockart Jr., *J. Virol.* **7**, 792 (1971).
28. K. Simons and E. Ikonen, *Nature* **387**, 569 (1997).
29. R. Xavier, T. Brennan, Q. Li, C. McCormack, B. Seed, *Immunity* **8**, 723 (1998).
30. Detergent-free caveolae fractions were prepared as described [E. J. Smart, Y. S. Ying, C. Mineo, R. G. Anderson, *Proc. Natl. Acad. Sci. U.S.A.* **92**, 10104 (1995); C. Mineo, G. L. James, E. J. Smart, R. G. Anderson, *J. Biol. Chem.* **271**, 11930 (1996)]. The reversibility of the effects of filipin treatment was investigated as described [J. E. Schnitzer, P. Oh, E. Pinney, J. Allard, *J. Cell. Biol.* **127**, 1217 (1994); R. Xavier, T. Brennan, Q. Li, C. McCormack, B. Seed, *Immunity* **8**, 723 (1998)]. Briefly, MEFs treated with filipin (Sigma) for 10 min were washed, incubated for 60 min in Dulbecco's modified Eagle's medium containing 20% fetal calf serum, and then stimulated with IFN-γ.
31. M. Sato *et al.*, *FEBS Lett.* **441**, 106 (1998).
32. A. Takaoka *et al.*, *EMBO J.* **18**, 2480 (1999).
33. Preparation of whole-cell extracts, binding reactions, and gel electrophoresis were done as described [A. Takaoka *et al.*, *EMBO J.* **18**, 2480 (1999)]. Unless otherwise noted, cells were treated with IFN-γ (250 U/ml) for 30 min. Equal amounts of proteins from whole-cell extracts were loaded onto each lane. Experiments were done in triplicate and were performed separately with at least two independent clones of MEFs derived from the same littermates of the WT or mutant mice.
34. After the treatment with IFN-γ (250 U/ml) for 15 min, cell lysis, immunoprecipitation, and immunoblotting were done as described [A. Takaoka *et al.*, *EMBO J.* **18**, 2480 (1999)]. The following antibodies were purchased: anti-phosphotyrosine, anti-Jak1, and anti-Jak2 (Upstate Biotechnology); anti-Stat1 p84/p91 and anti-Stat2 (Santa Cruz); anti-phosphorylated Stat1 (Tyr^{701}) (New England BioLabs); anti-IFNAR1, anti-IFNGR1, and anti-IFNGR2 (Research Diagnostics); and anti-caveolin (Transduction Laboratories).

35. We thank G. Uzé for the murine IFNAR1 cDNA (GenBank accession number M89041); J. Vilcek and E. L. Barsoumian for invaluable advice; M. Asagiri, N. Hata, Y. Kato, and S. H. Kim for technical support; Sumitomo Pharmaceuticals for purified murine IFN-α; and Toray Industries for recombinant murine IFN-β. Animal care was in accordance with institutional guidelines of the University of Tokyo. Supported by grants from the Research for the Future Program (96L00307), Yamanouchi Foundation for Research on Metabolic Disorders, the Japan Society for the Promotion of Science, Advanced Research on Cancer, and the Human Frontier Science Program Organization.

9 February 2000; accepted 2 May 2000

Perception of Brassinosteroids by the Extracellular Domain of the Receptor Kinase BRI1

Zuhua He,[1,3,4] Zhi-Yong Wang,[1] Jianming Li,[1]* Qun Zhu,[1]† Chris Lamb,[1]‡ Pamela Ronald,[3] Joanne Chory[1,2]§

An assay was developed to study plant receptor kinase activation and signaling mechanisms. The extracellular leucine-rich repeat (LRR) and transmembrane domains of the *Arabidopsis* receptor kinase BRI1, which is implicated in brassinosteroid signaling, were fused to the serine/threonine kinase domain of XA21, the rice disease resistance receptor. The chimeric receptor initiates plant defense responses in rice cells upon treatment with brassinosteroids. These results, which indicate that the extracellular domain of BRI1 perceives brassinosteroids, suggest a general signaling mechanism for the LRR receptor kinases of plants. This system should allow the discovery of ligands for the LRR kinases, the largest group of plant receptor kinases.

Receptor kinases mediate extracellular signals for diverse processes in plants and animals. Detailed mechanistic studies of both receptor tyrosine kinases and receptor serine/threonine kinases have been well documented in animal cells, where it has been shown that ligand binding to the extracellular domains of receptors induces receptor dimerization and stimulates receptor phosphorylation, resulting in the activation of intracellular signaling cascades (*1*–*3*). In contrast, the study of plant receptor-like kinases (RLKs), all of which are serine/threonine kinases, is still in its infancy (*4*, *5*). Despite the large numbers of putative RLKs encoded in the genomes of plants, how these receptors carry out signal transduction has yet to be determined.

Of the various RLKs, the largest group is the leucine-rich repeat receptor kinases (LRR-RLKs). This class consists of at least 120 genes in *Arabidopsis*. A few LRR-RLKs are involved in diverse biological processes based on their

[1]Plant Biology Laboratory, [2]The Howard Hughes Medical Institute, The Salk Institute for Biological Studies, La Jolla, CA 92037, USA. [3]Department of Plant Pathology, University of California, Davis, CA 95616, USA. [4]Biotechnology Institute, Zhejiang University, Hangzhou 310029, China.

*Present address: Department of Biology, University of Michigan, MI 48190–1048, USA.

† Present address: Dupont Company, Wilmington, DE 19880–0402, USA.

‡ Present address: John Innes Centre, Norwich, NR4 7UH, UK.

§To whom correspondence should be addressed. E-mail: chory@salk.edu